"©1996 IEEE. Personal use of this material is permitted. However, permission to reprint/republish this material for advertising or promotional purposes or for creating new collective works for resale or redistribution to servers or lists, or to reuse any copyrighted component of this work in other works must be obtained from the IEEE."

Evaluation of the Exact Union Bound for Trellis-Coded Modulations Over Fading Channels

C. Tellambura

***Abstract*—An analytical technique is presented for computing the exact union bound on the average bit error probability of trellis coded modulation schemes over Rayleigh, Rician, or shadowed Rician-fading channels. To this end, an integral expression is derived for the pairwise error event probability (PEP). Existing bounds can be obtained as special cases of this expression. It turns out that a Gauss–Chebysev quadrature rule offers excellent accuracy for this integral. By extension, the exact union bound (i.e., the weighted sum of all exact PEP's of a code) can readily be evaluated. This method has the same complexity as the union-Chernoff bound, and a few examples are given to show its application.**

I. Introduction

THE USE of trellis-coded modulation (TCM) in Gaussian channels confers power and bandwidth efficiency [1], and its use over mobile fading channels has recently received considerable attention. Accurate performance evaluation of TCM schemes is often needed, and the most useful performance measure is the *average bit-error probability* P_b.

The standard approach bounds P_b using a union bound (an infinite series)

$$P_b \leq \frac{1}{k} \sum_{\boldsymbol{z},\hat{\boldsymbol{z}} \in \mathcal{C}} a(\boldsymbol{z} \rightarrow \hat{\boldsymbol{z}}) P(\boldsymbol{z} \rightarrow \hat{\boldsymbol{z}}) \tag{1}$$

where k is the number of input bits per encoding interval, the pairwise error event probability (PEP) $P(\boldsymbol{z} \rightarrow \hat{\boldsymbol{z}})$ is the probability that the decoder selects the sequence $\hat{\boldsymbol{z}} \neq \boldsymbol{z}$ the transmitted sequence, $a(\boldsymbol{z} \rightarrow \hat{\boldsymbol{z}})$ is the number of bit errors due to this event, and $\mathcal{C}$ is the set of all legitimate code sequences.

To evaluate the union bound requires the Chernoff bound for each PEP. A transfer function, derived from a state diagram, enumerates all possible PEP's in a closed form, allowing the evaluation of an upper bound on P_b (hereafter referred to as the union-Chernoff bound). That is to say, one finds a Chernoff bound of the form

$$P(\boldsymbol{z} \rightarrow \hat{\boldsymbol{z}}) \leq \prod_n f(z_n, \hat{z}_n)$$

where z_n and $\hat{z}_n$ are the components of $\boldsymbol{z}$ and $\hat{\boldsymbol{z}}$, respectively. This, when used in conjunction with (1), yields the union-Chernoff bound. Clearly, the union-Chernoff bound bounds the right-hand side of (1). For fading channels, the Chernoff bound is slack (e.g., 4 dB away from the exact solution for a length two error event in Rayleigh fading), resulting in a loose upper bound on P_b. This drawback leads to a search for tighter upper bounds. A tight bound on the PEP, derived in [2] and [3], is asymptotically identical to the exact PEP and differs from the Chernoff bound only by a multiplier less than unity. Another technique [4] derives an exact expression for the PEP. This method cannot be used with the transfer function approach as it involves evaluating the m most significant terms of the union bound (1). Since it ignores the tail (the remaining terms), it yields a close approximation to P_b at high SNR's (signal-to-noise ratios), not an upper bound. By bounding the tail with a union-Chernoff bound, [5] offers a hybrid solution.

This paper provides a method to evaluate the *exact* union bound on P_b. That is, an exact expression for the PEP is used in the union bound (1), not an upper bound. To achieve this, a new integral expression for the PEP is derived, which generalizes most of the previous work. This method applies to TCM transmitted over Rayleigh, Rician, or shadowed Rician-fading channels using coherent detection with ideal channel state information (CSI) and ideal interleaving. Special cases of the integral expression include the Chernoff bound [6], the bound [3], and an approximation [7]. Our results show that the bound [3] can also be extended to Rician channels.

In the following, a rate 2/3, four-state 8PSK trellis code [8] is used as an example. The trellis diagram of this code is shown in Fig. 1. Its bitwise input $(b_k^{(1)}, b_k^{(2)})$ and output $(c_k^{(1)}, c_k^{(2)}, c_k^{(3)})$ relationship is [5]

$$\begin{aligned} c_k^{(1)} &= b_{k-1}^{(2)} \\ c_k^{(2)} &= b_k^{(1)} \\ c_k^{(3)} &= b_{k-1}^{(1)} \oplus b_k^{(2)}. \end{aligned}$$

The following model and simplifying assumptions are used. For an input M-ary phase shift keying (MPSK) symbol z_n (i.e., $z_n \in \{\exp(j2\pi k/M) | k = 0, 1, \cdots, M-1\}$ and $j = \sqrt{-1}$), the channel output is [9]

$$y_n = a_n z_n + v_n$$

where a_n is a fading amplitude, and v_n is a Gaussian noise sample. The following are assumed.

A1: The a_n's are independent and identically distributed random variables (i.e., ideal interleaving/deinterleaving).

A2: Each a_n remains constant during a symbol interval (i.e., nonselective slow fading).

Paper approved by T. Aulin, the Editor for Coding and Communication Theory of the IEEE Communications Society. Manuscript received January 1, 1996; revised June 5, 1996.

The author is with Telecommunications Research Group, Department of Electronic Engineering, University of Bradford, Bradford, West Yorkshire, U.K.

Publisher Item Identifier S 0090-6778(96)09029-0.

0090–6778/96$05.00 © 1996 IEEE

Authorized licensed use limited to: UNIVERSITY OF ALBERTA. Downloaded on December 23, 2009 at 18:10 from IEEE Xplore. Restrictions apply.

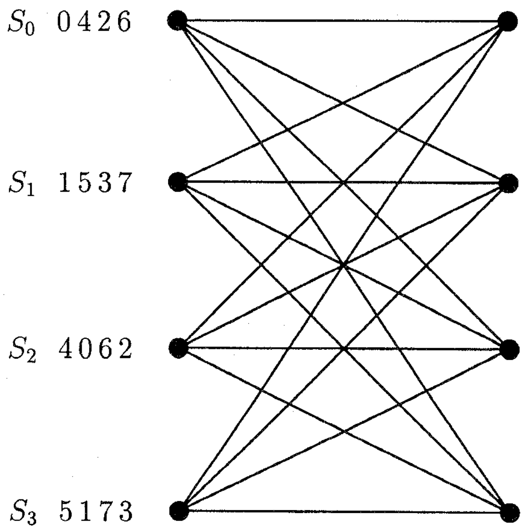

Fig. 1. Rate 2/3 four-state convolutional encoder.

A3: The receiver has ideal CSI (i.e., a_n is known to the receiver).

II. Independent Rayleigh Fading

Since each fading amplitude a_n is Rayleigh-distributed, the power variable $u = a_n^2$ has a chi-square probability distribution with two degrees of freedom. Thus, its moment generating function (MGF) $E\{e^{-su}\}$ is [10]

$$M_u(s) = \frac{1}{(s+1)}. \tag{2}$$

Consider two codewords $\boldsymbol{z} = \{z_1, z_2, \cdots, z_N\}$ and $\hat{\boldsymbol{z}} = \{\hat{z}_1, \hat{z}_2, \cdots, \hat{z}_N\}$ of length N. The PEP conditional on the fading amplitude sequence $\boldsymbol{a} = \{a_1, a_2, \cdots, a_N\}$ is [9]

$$P(\boldsymbol{z} \to \hat{\boldsymbol{z}} | \boldsymbol{a}) = \tfrac{1}{2} \operatorname{erfc}\left(\sqrt{\sum_{n \in \eta} a_n^2 \delta_n^2}\right) \tag{3}$$

where $\eta \triangleq \{n: z_n \neq \hat{z}_n, n = 1, \cdots, N\}$, $\delta_n^2 \triangleq \gamma_s |z_n - \hat{z}_n|^2/4$, and $\gamma_s = \overline{E}_s/N_0$ is the average signal-to-noise ratio. Let the number of elements of η be L and $L \le N$. The problem is to find the average of the above over the $\{a_n\}$.

The complementary error function has an integral definition [11, 7.4.11]:

$$\operatorname{erfc}(a) = \frac{2}{\pi} \int_0^\infty \frac{e^{-a^2(t^2+1)}}{t^2+1}\, dt. \tag{4}$$

By combining (3) and (4) the conditional PEP can be expressed as an integral. Thus, with $E(x)$ denoting the average of x, one gets

$$P(\boldsymbol{z} \to \hat{\boldsymbol{z}}) = \frac{1}{\pi} E\left[\int_0^\infty \frac{\exp\left[-(t^2+1)\sum_{n\in\eta} a_n^2 \delta_n^2\right]}{t^2+1}\, dt\right]$$

$$= \frac{1}{\pi} \int_0^\infty \frac{1}{t^2+1} \prod_{n \in \eta} \frac{1}{1 + \delta_n^2(t^2+1)}\, dt \tag{5}$$

since the first integrand is the product of the factors $\exp[-a_n^2\delta_n^2(t^2+1)]$, and since the average of each factor follows from (2). The second expression is the exact PEP as an integral. For a given sequence of δ_n, one can use partial factors and evaluate each integral, and that would be equivalent to the residue method given in [4].

The above can be approximated with a Gauss-Chebysev quadrature formula, and details are given in the Appendix, leading to the following:

$$P(\boldsymbol{z} \to \hat{\boldsymbol{z}}) = \frac{1}{2m} \sum_{j=1}^{m} \prod_{n \in \eta} \frac{1}{1 + \delta_{nj}^2} + R_m \tag{6}$$

where $\delta_{nj}^2 \triangleq \delta_n^2 \sec^2[(2j-1)\pi/4m]$ and m is a small positive integer. As m increases the remainder term R_m becomes negligible, as demonstrated by the example below and the bounds in the Appendix, where it is shown that $|R_m| \le \kappa_1 \gamma_s^{-2m}$ as $\gamma_s \to \infty$ for some κ_1.

Example 1: Consider an error event with the squared distance set of $\{2, 4\}$, which is the shortest error event of Ungerboeck's eight-state 8PSK trellis code [4]. Consider its reception in a Rayleigh fading channel with perfect CSI. For this error event, Table I compares the summation formula (6) and the exact PEP, derived in [4, eq. (29)]. The excellent accuracy of (6) is evident; for example, even the two-point sum is exact at 20 dB. Further numerical experiments for other error events confirm that (6) is very accurate in all cases, but for longer error events, (i.e., $L > 2$) it may be necessary to use slightly larger m values; however, $m = 5$ appears to be enough for most error events (then the error term vanishes with γ_s^{-10} for $\gamma_s \to \infty$).

TABLE I
PEP on Rayleigh Fading

γ_s (dB)	Exact	m = 2	4	5
0	8.16×10^{-2}	7.98×10^{-2}	8.16×10^{-2}	8.16×10^{-2}
5	1.97×10^{-2}	1.96×10^{-2}	1.97×10^{-2}	1.97×10^{-2}
10	3.0×10^{-3}	3.0×10^{-3}	3.0×10^{-3}	3.0×10^{-3}
15	3.4716×10^{-4}	3.4711×10^{-4}	3.4716×10^{-4}	3.4716×10^{-4}
20	3.6581×10^{-5}	3.6581×10^{-5}	3.6581×10^{-5}	3.6581×10^{-5}

Since the explicit evaluation of (5) is made difficult by the presence of the factors $1 + \delta_n^2(t^2+1)$ in the denominator, it is possible to simplify these factors to get some upper bounds, as considered in the following examples.

A. Chernoff Bound

Clearly, since $1 + \delta_n^2(t^2+1) \ge 1 + \delta_n^2$ for real t, one has from (5)

$$P(\boldsymbol{z} \to \hat{\boldsymbol{z}}) \le \left(\frac{1}{\pi}\int_0^\infty \frac{1}{t^2+1}\, dt\right) \prod_{n\in\eta} \frac{1}{1+\delta_n^2}$$

$$\le \frac{1}{2} \prod_{n \in \eta} \frac{1}{1 + \delta_n^2}. \tag{7}$$

Authorized licensed use limited to: UNIVERSITY OF ALBERTA. Downloaded on December 23, 2009 at 18:10 from IEEE Xplore. Restrictions apply.

This is the familiar Chernoff bound on the PEP and was first derived in [6]. The atypical derivation[1] of this paper reveals why the Chernoff bound is slack. For long error events ($L \gg 1$), the integrand in (5) decays rapidly and the main contribution to the integral arises from the vicinity of $t = 0$. Then, neglecting t in the denominator infuses a relatively less error. However, for most TCM schemes $L_{\min} = 2$ and the Chernoff bound is, therefore, weakest for such codes, improving as L increases.

B. Asymptotic Bound

Revisiting (5), since $1 + \delta_n^2(t^2+1) > \delta_n^2(t^2+1)$, one finds that

$$\begin{aligned} P(\boldsymbol{z} \to \hat{\boldsymbol{z}}) &< \frac{1}{\pi}\int_0^\infty \frac{1}{t^2+1}\prod_{n\in\eta}\frac{1}{\delta_n^2(t^2+1)}\,dt \\ &< \left(\frac{1}{\pi}\int_0^\infty \frac{1}{(t^2+1)^{L+1}}\,dt\right)\prod_{n\in\eta}\frac{1}{\delta_n^2} \\ &< B(L)\prod_{n\in\eta}\frac{1}{\delta_n^2} \end{aligned} \tag{8}$$

where

$$B(L) \triangleq \frac{1}{\pi}\int_0^\infty \frac{1}{(t^2+1)^{L+1}}\,dt = \frac{1}{4^L}\binom{2L-1}{L}.$$

Equation (8) is identical to [7, eq. (3)]. In [3] and [7], it is described as an "approximation," but clearly it is a *true upper bound*. Under asymptotic conditions ($\gamma_s \gg 1$), it is tighter than the Chernoff bound by the factor $B(L)$.

C. Another Upper Bound

Let $x_n \triangleq \sqrt{\delta_n^2/(1+\delta_n^2)}, x_{\min} = \min\{x_n : n \in \eta\}$ and $x_{\max} = \max\{x_n : n \in \eta\}$. Thus

$$\begin{aligned} P(\boldsymbol{z} \to \hat{\boldsymbol{z}}) &= \frac{1}{\pi}\int_0^\infty \frac{1}{(t^2+1)}\prod_{n\in\eta}\frac{1}{(x_n^2t^2+1)(1+\delta_n^2)}\,dt \\ &< I(L, x_{\min})\prod_{n\in\eta}\frac{1}{1+\delta_n^2} \end{aligned} \tag{9}$$

where

$$\begin{aligned} I(L, x_{\min}) &= \frac{1}{\pi}\int_0^\infty \frac{1}{(t^2+1)(x_{\min}^2t^2+1)^L}\,dt \\ &= \frac{1}{4^L}\sum_{k=0}^{L-1}\binom{L-1+k}{k}\left(\frac{2}{1+x_{\min}}\right)^{L-k}. \end{aligned}$$

This bound (9) is derived in [2] and [3] following a completely different approach, with a recursive formula for $I(L, x)$ given in [3, (B.3)]. Here, $I(L, x)$ has been derived using the formula for the error performance of binary PSK with Lth-order diversity in Rayleigh fading [10, 7.4.15]. Moreover, since the derivation of (9) rests on the inequality

$$\prod_{n\in\eta}(x_n^2t^2+1) \geq (x_{\min}^2t^2+1)^L$$

several observations about the tightness of the upper bound can be made, as shown below.

1) The bound is tightest for the $L = 2$ case and relatively loosens as L increases.
2) The tightness of the bound improves if there are repeated values in the set $\{|z_n - \hat{z}_n|^2 : n \in \eta\}$.
3) Asymptotically with γ_s, the bound is identical (regardless of the value of L) to the exact PEP. This follows from the fact that as $\gamma_s \to \infty, x_n \to 1\ \forall n$. Thus, $x_{\min} \approx x_{\max} \approx 1$.

Since $x_{\min} < 1 (x_{\min} \to 1$ as $\gamma_s \to \infty)$, it follows that

$$I(L, x_{\min}) < \frac{1}{4^L}\binom{2L-1}{L}.$$

This coupled with the bound (9) leads to (8). Thus, the differences between the bounds (8) and (9) are minor in terms of accuracy.

D. Union Bound

Consider the exact evaluation of the union bound (1). Let $\boldsymbol{Z} = (Z_1, Z_2, \cdots)$ be a vector of formal variables. Define the generating function of the form

$$T(\boldsymbol{Z}, I) = \sum_{\boldsymbol{z},\hat{\boldsymbol{z}}\in C} I^{a(\boldsymbol{z}\to\hat{\boldsymbol{z}})}\prod_{n\in\eta} Z_n \tag{10}$$

where I is another formal variable. Moreover, let

$$D_n(t) \triangleq \frac{1}{1+\delta_n^2(t^2+1)}.$$

The number of distinct values that $D_n(t)$ can take depends on the size of the signal constellation. The transfer function $T(\boldsymbol{D}(t), I)$ can be determined by the usual techniques.[2] For instance, a signal flow graph may be used with the branch labels of the form $I^v D_n(t)$. By contrast, for the union-Chernoff bound, the branches are labeled with $I^v(1+\delta_n^2)^{-1}$, resulting in the usual transfer function bound [5].

Combining (1), (5), and (10), and using the standard analysis [14], one obtains

$$P_b \leq \frac{1}{k\pi}\frac{\partial}{\partial I}\left\{\int_0^\infty \frac{1}{t^2+1}T(\boldsymbol{D}(t), I)\,dt\right\}\Bigg|_{I=1}. \tag{11}$$

It is interesting to note that the union-Chernoff bound is obtained by simply replacing the integral with the integrand evaluated at $t = 0$. Moreover, the use of Ostrowski's inequality of integrals for monotonic functions [15] shows

$$\int_0^\infty \frac{1}{t^2+1}T(\boldsymbol{D}(t), I)\,dt \leq \frac{\pi}{2}T(\boldsymbol{D}(0), I)$$

[1] For a continuous random variable $\boldsymbol{x}$ denoting the metric difference, the Chernoff bound is given as: $P(x \geq 0) \leq E\{e^{\lambda x}\}$ where $\lambda \geq 0$ is to be optimized to yield the tightest bound. For example, in [6], $E\{e^{\lambda x}|\boldsymbol{a}\}$ is optimized first, and the result is averaged over the probability distribution of $\boldsymbol{a}$ to bound the unconditional probability, $P(x \geq 0)$.

[2] In general, however, coded modulation schemes are nonlinear (i.e., P_b depends on the transmitted sequence). A research topic in its own right, this topic is not treated further here. We simply assume that the trellis code under consideration is uniform [12], [13].

Authorized licensed use limited to: UNIVERSITY OF ALBERTA. Downloaded on December 23, 2009 at 18:10 from IEEE Xplore. Restrictions apply.

where the right-hand side is the transfer function associated with the union-Chernoff bound. The bound (11) can readily be evaluated via a suitable numerical method. But it is simpler to use the summation formula (A.3). Since $T(\boldsymbol{D}(t), I)$ is a function of t^2+1, one has

$$T(\boldsymbol{D}(t), I) = \psi(t^2+1, I).$$

Using the method in the Appendix, the union bound is evaluated as

$$P_b \le \frac{1}{2mk}\frac{\partial}{\partial I}\left\{\sum_{j=1}^{m}\psi\left(\sec^2\left(\frac{2j-1}{4m}\right), I\right)\right\}\Bigg|_{I=1} \qquad (12)$$

where the partial derivative can be computed as the normalized first difference [14].

Example 2: Consider the reception of rate 1/2, two-state trellis-coded QPSK in Rayleigh fading. This coded modulation is analyzed in [16, Example 9.1], which treats both asymmetric and symmetric QPSK signal sets. However, for simplicity, only the symmetric case (i.e., signal points are $\exp(jn\pi/2), j=\sqrt{-1}, n=0,\cdots,3$) is considered here. Using branch label gains, $D_n(t)$, the transfer function becomes

$$T(\boldsymbol{D}(t), I) = \frac{2I}{(1+\gamma_s(t^2+1))(2-2I+\gamma_s(t^2+1))}.$$

Substituting this in (11), carrying out the integration, and evaluating the derivative at $I=1$, one has

$$P_b \le 1 - \frac{1}{2\gamma_s} + \frac{3}{4\gamma_s^2} - \sqrt{\frac{\gamma_s}{1+\gamma_s}}. \qquad (13)$$

This is the exact union bound for this coded modulation. By contrast, the union-Chernoff bound for this case is found to be [16, eq. (9.45)]

$$P_b < \frac{2(2+\gamma_s)}{\gamma_s^2(1+\gamma_s)}. \qquad (14)$$

Asymptotically, the right-hand side of (13) tends to $3/8\gamma_s^2$, while that of (14) tends to $2/\gamma_s^2$. This implies that the union-Chernoff bound is away from the exact union bound by 3.6 dB at high SNR's, and about a 4 dB difference can be observed between the union-Chernoff bound and the simulation results [16, Fig. 9.7].

Example 3: Consider the trellis-coded 8PSK scheme, whose trellis diagram is shown in Fig. 1. Since the modified transfer function (based on the union-Chernoff bound) is derived in detail elsewhere [5], the same results can be used, the only difference being that the weight profiles are obtained using $D_n(t)$, not $D_n(0)$. The modified transfer function is given as

$$T(\boldsymbol{D}(t), I) = \epsilon_1\alpha_{13} + \epsilon_2\alpha_{14} + \epsilon_3\alpha_{15} \qquad (15)$$

where

$$\begin{bmatrix}\epsilon_1\\ \epsilon_2\\ \epsilon_3\end{bmatrix} = \begin{bmatrix}1-\alpha_4 & -\alpha_{10} & -\alpha_8\\ -\alpha_9 & 1-\alpha_5 & -\alpha_{12}\\ -\alpha_7 & -\alpha_{11} & 1-\alpha_6\end{bmatrix}^{-1}\begin{bmatrix}\alpha_1\\ \alpha_2\\ \alpha_3\end{bmatrix}$$

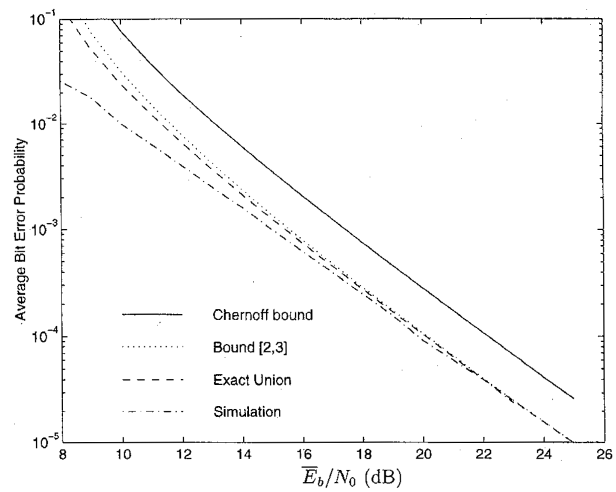

Fig. 2. The performance of the four-state 8PSK TCM [8] in Rayleigh fading with perfect CSI and ideal interleaving.

and the branch gain are given as

$$\begin{aligned}
&\alpha_1 = ID_4(t) && \alpha_8 = ID_1(t)\\
&\alpha_2 = \alpha_5 = ID_2(t) && \alpha_{10} = I\\
&\alpha_3 = I^2D_2(t) && \alpha_{11} = I^2D_2(t)\\
&\alpha_4 = ID_3(t) && \alpha_{13} = D_1(t)\\
&\alpha_6 = \alpha_7 = 0.5I^2(D_1(t)+D_3(t)) && \alpha_{14} = D_4(t)\\
&\alpha_9 = \alpha_{12} = 0.5I(D_1(t)+D_3(t)) && \alpha_{15} = D_3(t).
\end{aligned}$$

Recall the definition $\delta_n^2 \triangleq \gamma_s|z_n - \hat{z}_n|^2/4$. For this code, the set of values of $|z_n - \hat{z}_n|^2$ is $\{2-\sqrt{2}, 2, 2+\sqrt{2}, 4\}$, and $D_n(t)$ $(n=1,\cdots,4)$ have been calculated using this set of squared distances. Based on the above, the exact union bound on P_b is plotted in Fig. 2 as a function of $\overline{E}_b/N_0$ (for this code, $\overline{E}_s = 2\overline{E}_b$). For this calculation, the two expressions have been compared: (11) evaluated using numerical integration (seven-figure accuracy) and the summation formula (12) with $m=5$. Both methods yield virtually the same answer for the considered range of SNR's. Simulation results, the union-Chernoff bound, and the bound (9) with the transfer function approach [2, Theorem 2] are also shown in this figure. The general weakness of the Chernoff bound is clearly evident. However, the union-Chernoff bound is almost parallel to the exact union bound. Thus the gap can be bridged by some sort of tightening factor. (9) achieves this goal. Finally, the exact union bound itself becomes rather loose for low signal-to-noise ratios (SNR's).

III. Rician Fading

Now the distribution of the variable $u = a_n^2$ relates to the noncentral chi-square distribution. Its MGF can be shown to be [10]

$$M_u(s) = \frac{1+K}{1+K+s}\exp\left(-\frac{Ks}{1+K+s}\right) \qquad (16)$$

where K represents the ratio of average power in the line-of-sight (LOS) over that in the scattered component. Typical

Authorized licensed use limited to: UNIVERSITY OF ALBERTA. Downloaded on December 23, 2009 at 18:10 from IEEE Xplore. Restrictions apply.

values of K for the mobile satellite channel are $5 \sim 10$ dB. By employing a derivation similar to that used for (5), one finds

$$P(z \to \hat{z}) = \frac{1}{\pi} \int_0^{\infty} \frac{1}{t^2+1} \left(\prod_{n \in \eta} M_u(\delta_n^2(t^2+1)) \right) dt. \tag{17}$$

As previously, this is the exact PEP as an integral, and for $K = 0$, it reduces to the Rayleigh case (5).

To evaluate the exact union bound follows the same approach as in Section II. Either (11) or (12) can be used, and the only difference is that the branch gains now take the form

$$D_n(t) \triangleq \frac{1+K}{1+K+\delta_n^2(t^2+1)} \cdot \exp\left(-\frac{K\delta_n^2(t^2+1)}{1+K+\delta_n^2(t^2+1)}\right).$$

Before proceeding further, note that an upper bound akin to (9) can be obtained. For $t \geq 0$

$$M_u(\delta_n^2(t^2+1)) < \frac{1+K}{1+K+\delta_n^2(t^2+1)} \exp\left(-\frac{K\delta_n^2}{1+K+\delta_n^2}\right)$$

and the first factor on the right-hand side is reminiscent of the Rayleigh fading case. This is evident if δ_n^2 is replaced by $(1+K)\delta_n^2$. Thus, (17) can be bounded by the product of an integral expression similar to (5) and constant exponential factors. In other words, t is set to zero in the exponential factors in the integrand (17) to yield a bound similar to (9). By following the method in Section II, one has

$$P(z \to \hat{z}) < I(L, \tilde{x}_{\min}) \prod_{n \in \eta} \frac{1+K}{1+K+\delta_n^2} \exp\left(-\frac{K\delta_n^2}{1+K+\delta_n^2}\right) \tag{18}$$

where $\tilde{x}_n \triangleq \sqrt{\delta_n^2/(1+K+\delta_n^2)}$. Note that the definition of $\tilde{x}_n$ encompasses the previous definition of x_n.

The integral (17) can be expressed as a sum by using a Gauss–Chebysev m-point integral formula, and the details are given in the Appendix. It follows that

$$P(z \to \hat{z}) = \frac{1}{2m} \sum_{j=1}^{m} \prod_{n \in \eta} M_u(\delta_{nj}^2) + R_m \tag{19}$$

where $\delta_{nj}^2 \triangleq \delta_n^2 \sec^2[(2j-1)\pi/4m]$. The remainder term R_m is negligible, as demonstrated by the example below and the bounds evaluated in the Appendix .

Example 4: Consider the shortest error event of Ungerboeck's eight-state 8PSK trellis code [4], used in Example 1, and its reception in a Rician fading channel ($K = 5$ dB) with perfect CSI. The exact expression for the PEP (17) is numerically computed to seven-figure accuracy in Table II, along with the summation formula (19). The excellent accuracy of (19) is evident; for example, even the two-point sum has an accuracy of 10^{-5} for SNR's greater than 10 dB. Further numerical experiments for other error events have confirmed that (19) is very accurate in all cases.

TABLE II
PEP ON RICIAN FADING

γ_s (dB)	Exact	m = 2	4	5
0	6.04×10^{-2}	5.96×10^{-2}	6.04×10^{-2}	6.04×10^{-2}
5	7.8×10^{-3}	7.9×10^{-3}	7.8×10^{-3}	7.8×10^{-3}
10	4.19×10^{-4}	4.203×10^{-4}	4.19×10^{-4}	4.19×10^{-4}
15	2.079×10^{-5}	2.078×10^{-5}	2.079×10^{-5}	2.079×10^{-5}
20	1.4365×10^{-6}	1.4362×10^{-6}	1.4365×10^{-6}	1.4365×10^{-6}

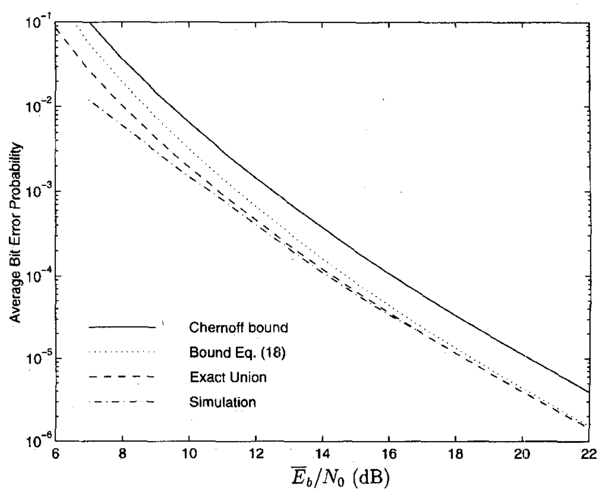

Fig. 3. The performance of the four-state 8PSK TCM [8] in Rician fading ($K = 5$ dB) with perfect CSI and ideal interleaving.

Example 5: Following a method similar to that of Example 3, the exact union bound on P_b for the same four-state 8PSK TCM scheme in Rician fading is plotted in Fig. 3. It is computed using the summation formula (12) with $m = 5$. Simulation results, the union-Chernoff bound, and the bound (18) with the transfer function approach [2, Theorem 2] are also shown in this figure. The general weakness of the Chernoff bound is evident. In this section (9) has been extended to the Rician case (17). In both Rayleigh and Rician cases, the bound achieves improved accuracy, but to a lesser degree for the Rician case.

IV. SHADOWED RICIAN FADING

The pdf of a shadowed Rician variable is [5], [17]

$$p(a) = \frac{2a}{b_0\sqrt{2\pi d_0}} \int_0^{\infty} \frac{1}{z} \exp[-q(z)] I_0\left(\frac{2az}{b_0}\right) dz; \quad a \geq 0$$

where $q(z) = (\ln z - \mu_0)^2/(2d_0) + (a^2+z^2)/b_0, z$ is the log-normal LOS component, i.e., $z = e^v$ and v is Gaussian with mean μ_0 and variance d_0. The scattered component in the signal is Rayleigh distributed with a mean squared value of $b_0/2$. $I_0(x)$ is the zero order modified Bessel function.

Authorized licensed use limited to: UNIVERSITY OF ALBERTA. Downloaded on December 23, 2009 at 18:10 from IEEE Xplore. Restrictions apply.

As before, our development needs the MGF. Thus

$$\begin{aligned} M_u(s) &= \int_0^\infty e^{-sa^2} p(a)\, da \\ &= \int_0^\infty \frac{d_1}{z} \exp\left[\frac{-(\ln z - \mu_0)^2}{2d_0}\right] \psi(z, s)\, dz \\ &= \sum_{j=1}^{p} w_j \psi(e^{\sqrt{2d_0}t_j + \mu_0}, s) + R_p \end{aligned} \tag{20}$$

where $d_1 = 1/\sqrt{2\pi d_0}$

$$\psi(z, s) \triangleq \frac{1}{\sqrt{\pi}(1 + b_0 s)} \exp\left(-\frac{z^2 s}{1 + b_0 s}\right)$$

R_p is a remainder term and p is a small positive integer. By integrating over a, the middle term in (20) is obtained. The third step is in fact the Gauss–Hermitian integral formula [11, 25.4.6] obtained by the substitution $t = (\ln z - \mu_0)/\sqrt{2d_0}$. The weights w_j and abscissas t_j for $p \le 20$ can be found in the same reference. R_p vanishes for large p values (e.g., $p \sim 10$).

Now the performance evaluation can proceed as before. The exact PEP is obtained via (17) or (19), and the branch gains take the form $D_n(t) = M_u(\delta_n^2(t^2 + 1))$ from (20).

Example 6: As previously, the exact union bound on P_b for a rate 2/3, eight-state 8 PSK TCM scheme in shadowed Rician fading is plotted in Fig. 4 as a function[3] of $\overline{E}_b/N_0$. This code is a well-known Ungerboeck code [1], and its encoder transfer function is derived in [5]. In developing the transfer function, the appropriate branch gains must be used (see above and Section III). For this computation, the summation formula (12) with $m = 5$ and a 20-point Hermite rule [i.e., $p = 20$ in (20)] have been applied. Simulation results and the union-Chernoff bound are also shown in this figure. Once again the general weakness of the Chernoff bound is evident. The exact union bound is very tight for $P_b \le 10^{-3}$, but gets rather loose for low SNR's.

V. Conclusion

In this paper, the exact union bounds on average bit-error probability of TCM schemes over Rayleigh, Rician, and shadowed Rician channels have been derived. To achieve this, the PEP has been expressed as an integral, and some existing results have been derived as special cases. The quadrature formula for this integral turns out to be remarkably accurate. The same formula can be used to compute the exact union bound on the performance.

The exact union bound is very accurate for $P_b \le 10^{-3}$, but for low SNR's it gets rather loose. Surprisingly, some previous bounds [2], [7] are as good as the exact union bound for high SNR's. The evaluation of the exact union bound, however, is no more complex than these methods. Our results can be extended to the diversity reception of TCM, in particular, for maximal ratio combining with ideal CSI [18].

[3] Unlike the case of Rayleigh or Rician-channel models, the mean $\overline{a^2}$ is not equal to unity for this model. This factor has been taken into account when the results were computed.

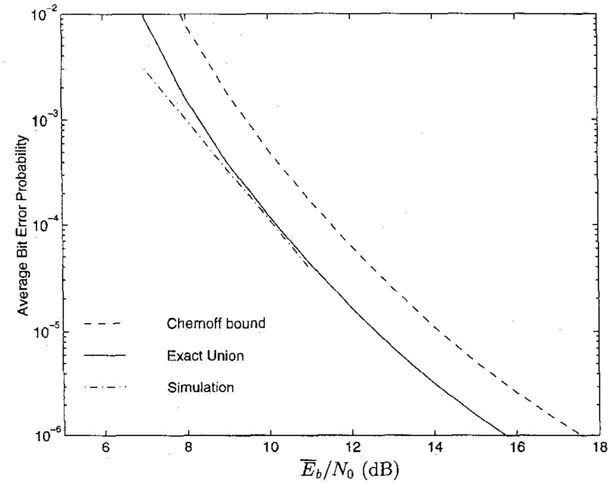

Fig. 4. The performance of an eight-state 8PSK TCM scheme [1] in a shadowed Rician fading channel with perfect CSI and ideal interleaving. The shadowed Rician fading parameters are [17]: $\sqrt{d_0} = 0.115, b_0/2 = 0.158$, and $\mu = 0.115$.

Appendix

Here, the approximation (6) is developed along with some error bounds. Consider the integral

$$I = \frac{1}{\pi} \int_0^\infty \frac{1}{t^2 + 1} f(t^2 + 1)\, dt. \tag{A.1}$$

Using the substitution $y = 1/(t^2 + 1)$, one has

$$I = \frac{1}{2\pi} \int_0^1 \frac{1}{\sqrt{y(1 - y)}} f(1/y)\, dy. \tag{A.2}$$

This can be reduced to [11, 25.4.38] using $2y - 1 = x$, which can be approximated by a Gaussian quadrature formula, using orthogonal Chebysev polynomials of first kind. Accordingly, one has

$$I = \frac{1}{2m} \sum_{j=1}^{m} f\left[\sec^2 \frac{(2j - 1)\pi}{4m}\right] + R_m \tag{A.3}$$

where R_m is a remainder term. It can be upper bounded [11, 25.4.38] to give

$$|R_m| \le \max_{-1<x<1} \frac{1}{(2m)! 2^{2m}} |f^{2m}(x)|. \tag{A.4}$$

Applying (A.3) to (5) can be done with the function

$$f(x) = \prod_{n \in \eta} \frac{1 + x}{1 + x + 2\delta_n^2} \tag{A.5}$$

for a given error event.

Using Maple, a popular computer algebra system, the bound (A.4) is calculated for error events with squared distance sets $\{2, 4\}$ and $\{2, 4, 4\}$ in Table III and Table IV, respectively. These values confirm the excellent accuracy of (A.3) in this case.

The right-hand side in (A.4) can also be bounded using the theory of analytic functions. Consider the complex $z\ (= x + iy)$

Authorized licensed use limited to: UNIVERSITY OF ALBERTA. Downloaded on December 23, 2009 at 18:10 from IEEE Xplore. Restrictions apply.

TABLE III
BOUND ON R_m

γ_s (dB)	m		
	2	4	5
5	5.46×10^{-4}	3.87×10^{-7}	9.74×10^{-9}
10	5.46×10^{-6}	3.87×10^{-11}	9.74×10^{-14}
15	5.46×10^{-8}	3.87×10^{-15}	9.74×10^{-19}

TABLE IV
BOUND ON R_m

γ_s (dB)	m		
	2	4	5
5	3.12×10^{-4}	3.66×10^{-7}	9.57×10^{-9}
10	3.12×10^{-6}	3.66×10^{-11}	9.57×10^{-14}
15	3.12×10^{-8}	3.66×10^{-15}	9.57×10^{-19}

plane and let $\overline{\rho} = \min\{2\delta_n^2 + 1 : n \in \eta\}$. Then $f(z)$ (A.5) is analytic in the region $|z| < \overline{\rho}$. It can be shown that [19]

$$\max_{-1<x<1} |f^{2m}(x)| \leq \frac{2m! L(C) M_C}{2\pi\delta^{2m+1}}$$

where C is any contour that contains the real line $-1 \leq x \leq 1$ in its interior, $L(C)$ is the length of C, M_C is the maximum modulus of $f(z)$ along C, and δ is the minimum distance from points of C to points of the segment $-1 \leq x \leq 1$. Take C as the circle $|z| = \rho, 1 < \rho < \overline{\rho}$. Then it can be shown that $M_C = \max |f(z)|$ occurs at $z = \pm\rho$. The peak at $z = -\rho$ becomes larger than the other as $\rho \rightarrow \overline{\rho}$. Therefore, since $\delta = \rho - 1$, one finds that

$$|R_m| \leq \min_{1<\rho<\overline{\rho}} \frac{1}{2^{2m+1}} \frac{\rho}{(\rho-1)^{2m+1-L}(\overline{\rho}-\rho)^L} \qquad \text{(A.6)}$$

assuming $2m + 1 > L$. Selecting $\rho = \hat{\rho}$ that maximizes the denominator, then $((2m+1)\hat{\rho} = \overline{\rho}(2m+1-L) + L)$, and

$$|R_m| \leq \kappa(m, L) \frac{\overline{\rho} + L(2m+1-L)^{-1}}{(\overline{\rho}-1)^{2m+1}}$$

where the constant

$$\kappa(m, L) \triangleq \frac{(2m+1)^{2m}}{2^{2m+1}(2m+1-L)^{2m-L}}.$$

Recalling the definition of $\overline{\rho}$, as $\gamma_s \rightarrow \infty$ implies $\overline{\rho} \rightarrow \infty$, one has

$$|R_m| \leq \kappa(m, L) \frac{1}{(\delta_{\min}\gamma_s)^{2m}}$$

where $\delta_{\min} \triangleq \min\{|z_n - \hat{z}_n|^2/2 : n \in \eta\}$.

ACKNOWLEDGMENT

The author wishes to thank the anonymous reviewers for their helpful comments and Dr. M. G. Parker for editing the manuscript.

REFERENCES

[1] G. Ungerboeck, "Channel coding with multilevel/phase signals," *IEEE Trans. Inform. Theory*., vol. 28, pp. 55–67, Jan. 1982.

[2] S. B. Slimane and Tho Le-Ngoc, "a tight upper bound on the error probability of coded modulation schemes in Rayleigh fading channels," in *PIMRC'93*, Yokohama, Japan, Sept. 1993, pp. 249–253.

[3] ——, "Tight bounds on the error probability of coded modulation schemes in Rayleigh fading channels," *IEEE Trans. Veh. Technol.*, vol. 44, no. 1, pp. 121–129, Jan. 1995.

[4] J. K. Cavers and P. Ho, "Analysis of the error performance of trellis coded modulations in Rayleigh fading channels," *IEEE Trans. Commun.*, vol. 40, pp. 74–83, Jan. 1992.

[5] R. G. McKay, E. Biglieri, and P. J. McLane, "Error bounds for trellis-coded MPSK on a fading mobile satellite channel," *IEEE Trans. Commun.*, vol. 39, pp. 1750–1761, Dec. 1991.

[6] D. Divsalar and M. K. Simon, "Trellis-coded modulation for 4800 to 9600 bps transmission over a fading satellite channel," *IEEE J. Select. Areas. Commun.*, vol. 5, pp. 162–175, Feb. 1987.

[7] K. Chan and A. Bateman, "The performance of reference-based M-ary PSK with trellis coded modulation in Rayleigh fading," *IEEE Trans. Veh. Technol.*, vol. 41, pp. 190–198, May 1992.

[8] S. G. Wilson and Y. S. Leung, "Trellis coded phase modulation on Rayleigh channels," in *Proc. 1987 Int. Conf. Commun*, June 1987, pp. 21.3.1–21.3.5.

[9] D. Divsalar and M. K. Simon, "The design of trellis coded MPSK for fading channels: performance criteria," *IEEE Trans. Commun.*, vol. 36, pp. 1004–1011, Sept. 1988.

[10] J. G. Proakis, *Digital Communications*. New York: McGraw-Hill, 1989.

[11] M. Abramovitz and I. A. Stegun, *Handbook of Mathematical Functions*. New York: Dover, 1972.

[12] E. Zehavi and J. K. Wolf, "On the performance of trellis codes," *IEEE Trans. Inform. Theory*., vol. 33, pp. 196–202, Mar. 1987.

[13] E. Biglieri and P. J. McLane, "Uniform distance and error probability properties of TCM schemes," *IEEE Trans. Commun.*, vol. 39, pp. 41–52, Jan. 1991.

[14] A. J. Viterbi and J. K. Omura, *Principles of Digital Communication and Coding*. New York: McGraw-Hill, 1979.

[15] I. S. Gradshteyn and I. M. Ryzhik, *Table of Integrals, Series, and Products*, 5th edn. New York: Academic, 1994.

[16] E. Biglieri, P. J. McLane, M. K. Simon, and D. Divsalar, *Introduction to Trellis-Coded Modulation with Applications*. New York: MacMillan, 1991.

[17] C. Loo, "A statistical model for a land mobile satellite link," *IEEE Trans. Veh. Technol.*, vol. 34, pp. 122–127, Aug. 1985.

[18] G. Femenias and R. Agusti, "Analysis of predetection diversity TCM-MPSK and postdetection diversity TCM-MDPSK systems on a Rayleigh fading channel," *IEEE Trans. Commun.*, vol. 43, no. 2/3/4, pp. 374–385, Feb. 1995.

[19] P. J. Davies and P. Rabinowitz, *Methods of Numerical Integration*, 2nd ed. New York: Academic, 1984.

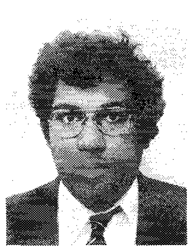

C. Tellambura received the B.Sc. degree in electronics and communications engineering from the University of Moratuwa, Sri-Lanka, in 1986, the MSc degree in electronics from the King's College, U.K., in 1988, and the Ph.D. degree in electrical engineering from the University of Victoria, Canada, in 1993.

He was with University of Moratuwa, Sri-Lanka from 1986 to 1987 and from 1988 to 1989, and the University of Victoria, Canada from 1993 to 1994. Presently, he is with the University of Bradford, U.K. His current research interests include indoor wireless communications.

Authorized licensed use limited to: UNIVERSITY OF ALBERTA. Downloaded on December 23, 2009 at 18:10 from IEEE Xplore. Restrictions apply.